ELSEVIER

PII: S0144-8617(96)00080-X

*Carbohydrate Polymers* **31** (1996) 105–112

0144-8617/96/$15.00 + .00

# Solution behaviour of cellulose and amylose in iron-sodiumtartrate (FeTNa)

**B. Seger, T. Aberle & W. Burchard**

*Institute of Macromolecular Chemistry, University of Freiburg, Sonnenstraße 5, 79104 Freiburg, FRG*

(Received 28 July 1995; revised version received 20 November 1995; accepted 28 November 1995)

Cellulose and amylose were examined by means of static and dynamic light scattering techniques. After discovering, that the metal complex solvent FeTNa dissolves these glucanes, a more detailed comparison of the solution properties was performed. In very dilute solutions cellulose and amylose exhibit semiflexible chain behaviour with no striking differences. The chain stiffness parameters were determined by analysing the angular dependence of the light scattering data obtained after extrapolation to zero concentration. Remarkable differences occurred, however, due to different H-bond systems, when increasing the polymer concentration beyond the overlap concentration $c^*$. In the case of amylose an entanglement network is built up mainly by single chains, which are temporarily fixed by reversible non-covalent bonds. Cellulose, on the other hand, seems to form a network consisting of fringed micellar aggregates, and only partially entangled flexible arms of these aggregates are maintained via H-bonds.


## INTRODUCTION

In the field of polysaccharide science cellulose holds an exceptional position as a framework substance in plant cellwalls and represents the world's most important renewable resource. The fibre formation is induced by the stretched chain conformation caused by the $\beta$-(1,4) glycosidic bond and a system of well organized H-bonds.

The corresponding $\alpha$-(1,4) glucan occurs in nature as amylose, and is one of the two components of starch, where the $\alpha$-linkage favours a helical structure. Both macromolecules exhibit complex suprastructures, a characteristic of all polysaccharides, where the various OH-groups are responsible for hydrogen bonding (Burchard, 1993).

Even in solution, these polymers exhibit a high tendency to associate, and the characterization of their solution behaviour gives serious problems. To study in isolation the influence of the different glycosidic bonds, all OH-groups had to be substituted to prevent H-bond formation. Such derivatives are obtained, for instance, by the reaction of cellulose and amylose with phenylisocyanate leading to the corresponding tri-carbanilates (Burchard, 1965). In the past, interest was focussed mainly on the determination of solution properties of such fully substituted derivatives. The lack of a common solvent has so far prevented a direct comparison of the unsubstituted cellulose and amylose in solution. Here we now present a common solvent for both polysaccharides and report results on the conformation.

In the 1950s, Jayme and Bergmann (1956) developed a series of metal complex solvent systems for cellulose, among which the iron tartaric acid complex (EWNN) was one of them. Subsequent to these studies Valtasaari (1957) developed a simplified modification of this solvent (FeTNa) and started an investigation of the solution properties of cellulose by means of viscometry and static light scattering (Valtasaari, 1971). To extend this work and for comparison with results using cuoxam as a solvent for cellulose (Seger & Burchard, 1994) we carried out light scattering measurements in FeTNa solutions. Improved precision of instrumental equipment for studying polymers in solution offered better possibilities for determining the solution properties, among others, the chain flexibility. Recently we discovered that FeTNa is also able to dissolve amylose to give molecularly dispersed solutions. Thus allowing direct comparison of cellulose and amylose.

The aim of this paper was to study the influence of the different glycosidic linkages on the chain dimensions and conformations, and determine the chain stiffness in the dilute concentration regime. In a second part we describe the transition to more concentrated solutions

and the association phenomena above the overlap concentration $c^*$.

## EXPERIMENTAL

### Materials

*Preparation of the solvent FeTNa (according to Valtasaari, 1957)*

FeTNa is a modification of the iron–sodium–tartrate solvent EWNN originally proposed by Jayme and Bergmann (1956). The advantages with respect to an investigation by means of light scattering are the lower salt content, lower solvent viscosity, lighter colour and exact reproducibility of the composition.

In a 1.5 litre beaker 0.9 mole sodiumtartrate dihydrate are dissolved by heating in 400 ml water. To avoid hydrolytic decomposition, the dissolution of 0.3 mole irontrinitrate monohydrate in water was done immediately prior to use. The mixing of the solutions was carried out under vigorous stirring and was protected from light. Precipitated tartrato-ferric acid could be redissolved by continous stirring. The solution was cooled down to a temperature of 10–15°C in an ice-water bath before adding 2.4 mole sodiumhydroxide dissolved in 200 ml of water. Since the complex-forming reaction is exothermic, the addition must be slow enough to avoid a temperature increase to more than 15–20°C. For complete complex formation about 75 ml of the alkali solution were consumed, indicated by a shift of the reddish-brown colour of the solution to yellowish-green; the rest of the alkali is added rapidly, disregarding any possible slight rise in temperature. Finally, the solution was transferred into a 1 litre flask, containing 5 g of sodium tartrate prescribed by Jayme and Bergmann (1956) for stabilization, and adjusted with water to the correct volume. The volume adjustment should be done as quickly as possible since the addition of water causes hydrolytic decomposition. The solution was filtered through a No. 4 glass filter after having been allowed to stand for at least 24 h. To remove small amounts of precipitated ferric hydroxide, the solution was centrifuged at 12 000 rpm for 30 min before use.

*Cellulose samples*

Measurements were performed with four hydrolyzed cotton linters species and five samples of pulp celluloses. All samples were unfractionated, the molar mass distribution of these degraded cotton celluloses was assumed to obey the Schulz–Flory most probable distribution.

*Amylose samples*

Amyloses were enzymatically synthesized from glucose-1-phosphate with isolated potato phosphorylase, using maltohexaose as primer (Pfannemüller & Burchard, 1969). The chain length was adjusted by the ratio of monomer to primer. Thus the molar mass distribution of these synthetic samples were assumed to be close to the Poisson distribution.

*Carbanilation*

To check the results of the measurements some cellulose and amylose samples were derivatized by reaction with phenylisocyanate in pyridine (Burchard & Husemann, 1961). As a modification of the described preparation of the triphenylurethan derivatives, a few drops of dibutyltin dilaureate were added as catalysts. To remove the products from the completely substituted substance an additional precipitation step of centrifuged dioxan solutions (30 000 rpm for 1 h) was introduced.

*Preparation of the solutions*

For the preparation of the solutions, the samples were dissolved in centrifuged FeTNa under $N_2$ atmosphere. They were well shaken and kept in the refrigerator until complete dissolution. The stock solutions (0.1% w/vol) were diluted at 20°C to five lower concentrations (down to 0.01% w/vol).

Solutions of higher concentration (from 1 to 5% w/vol) were produced in a high performance Büchi autoclave at 0–5°C because of the extremely high viscosity.

To remove any interfering particles from these solutions, the light scattering cells were centrifuged for one hour at 12 000 rpm. The floating technique of Dandliker and Kraut (1956) was applied, where the cells are floated in concentrated CsCl solution in the buckets of an ultracentrifuge rotor (Beckman L5-50 B, rotor SW-28).

*Light scattering measurements*

The light scattering measurements were performed with fully computerized and modified SOFICA photogoniometers (Baur, 1990). One was equipped with a He-Ne-laser ($\lambda_0 = 632.8$ nm) and the other with a Ar-ion-laser ($\lambda_0 = 488$ nm). The scattered light was recorded in an angular region from 30 to 145 degrees at steps of 5 degrees at a temperature of 20°C, using a refractive index $n_0$ of 1.384. The refractive index increment $dn/dc$ of 0.244 was determined by Valtasaari from dialyzed cellulosic solutions. For amylose we assumed the same value. Although the extinction of the light green FeTNa is sufficiently low, the absorption is not negligible and the results had to be corrected by means of UV-VIS-spectrometry (Perkin–Elmer).

In the case of more concentrated solutions also dynamic-light scattering measurements were carried out. Here the ALV photogoniometer (ALV-Langen, Hessen, Germany) was used, equipped with an ALV 5000 correlator/structurator. Because of the long recording time for one correlogramme (up to 7 h), the dynamic LS measurements were made only at 30°, 90° and 150° for a qualitative comparison.

## RESULTS AND DISCUSSION

### Dilute concentration regime

*Molecular parameters*

One of the intentions of the present study was the elucidation of the cellulose and amylose properties in dilute solution. Static light scattering (LS) was applied in FeTNa. The measurements involved some serious difficulties. These arose mainly from the solvent, that often contains larger aggregates of the FeTNa. These aggregates were eventually removed by ultracentrifugation. Despite the fact, that the sample cells were centrifuged before measurement, the light scattering data in Zimm plots still exhibit a marked angular dependence at low angles. This curvature is reduced with increasing centrifugation time as shown in Fig. 1. For the angular range above 70° linear $q^2$-dependence is observed, and the data for various centrifugation times do not differ any longer, indicating that no detectable concentration error was introduced by this floating technique. To eliminate the excess low angle scattering, resulting from this small amount of dispersed aggregates, a linear extrapolation to zero scattering angle of the data from the angular range between 70° and 145° was performed. An example is shown in Fig. 2.

By this method comparable results for the molar mass $M_w$, radius of gyration $R_g$ and second virial coefficient $A_2$ were obtained, as reported in literature for cellulose in FeTNa (Valtasaari, 1971). Furthermore, we checked by light scattering the degrees of polymerisation with the corresponding tri-carbanilate derivatives. Deviations were found to lie within limits of 6–16%. We therefore conclude, that the data represent single chain parameters.

A double logarithmic plot of the molecular weight dependence of the radii $R_g$ (Fig. 3) gave first information on the molecular structure. The relationship

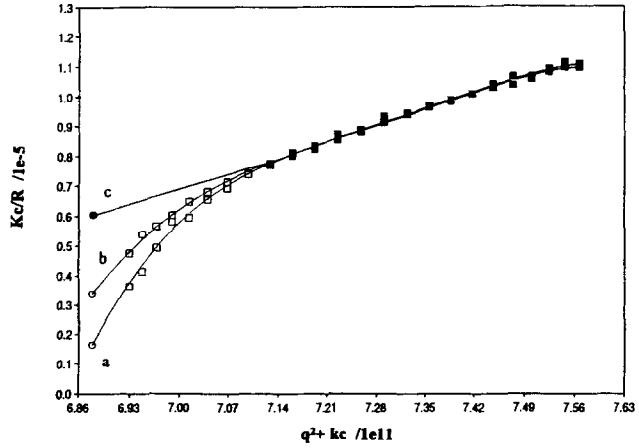


**Fig. 1.** Light scattering data (Zimm-plot) for concentration $c = 0.08$ w-% of the cellulose sample CEL-3 in FeTNa for different centrifuging times: (a) 30 min; (b) 2 h; (c) linear extrapolation of the angular range from 70–145°.

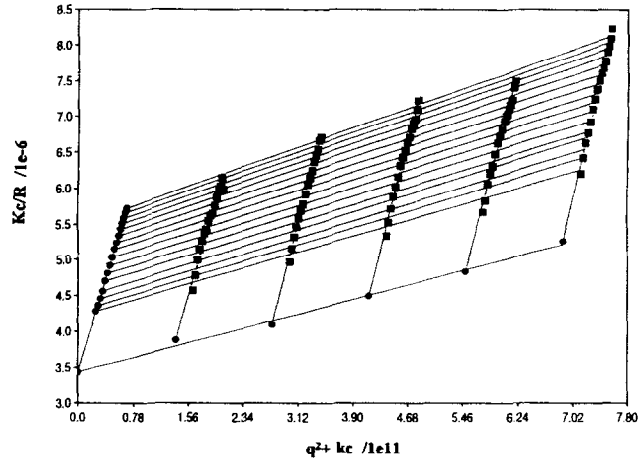


**Fig. 2.** Zimm-plot for amylose sample A-4 ($c = 0.02$–$0.1$ w-%). $q = (4\pi\eta_0/\lambda_0)\sin(\theta/2)$, where $\eta_0$ is the refractive index of the solvent, $\lambda_0$ the wavelength of the laser and $\theta$ the scattering angle.

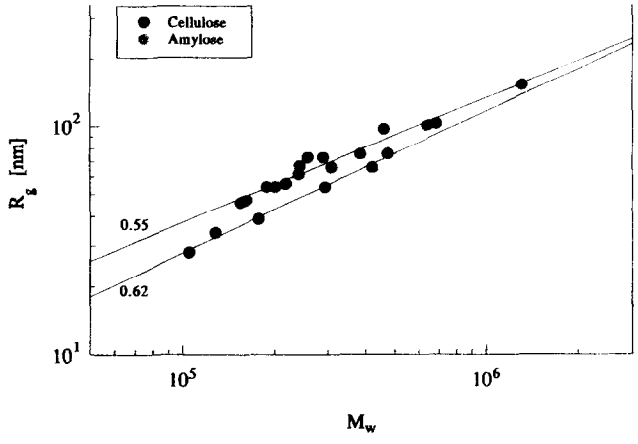


**Fig. 3.** Radius of gyration as a function of molar mass for cellulose and amylose in FeTNa.

between the radius of gyration $R_g = \langle S^2 \rangle_z^{1/2}$ and the molecular weight $M_w$ is commonly described by a power law

$$\langle S^2 \rangle \propto M^{a_s} \tag{1}$$

Such relationship holds also for cellulose and amylose in FeTNa, but apparently with different exponents. For cellulose an exponent $a_s = 2a_{Rg} = 1.1$ was obtained by combining our own results with data from literature (Valtasaari, 1971). For amylose, on the other hand, this exponent was found to be $a_s = 1.24$. These exponents are well in the range of good solvent behaviour ($a_s = 1.2$) of statistical coils. The obtained values indicate coil-like behaviour with a weak influence of chain stiffness for cellulose and amylose in dilute FeTNa solutions.

*Chain stiffness*

More detailed information on the chain stiffness could be obtained by a quantitative analysis of the LS data.

This was done by analysing the radius of gyration as a function of $M_w$ on the basis of the the Benoit–Doty relationship and by analysis of the angular dependence within the framework of the wormlike chain model.

The Benoit–Doty relationship (Benoit & Doty, 1953) expresses the mean square radius of gyration $\langle S^2 \rangle \equiv R_g^2$ in terms of the Kuhn segment length $l_k$ and number of such segments $N_k$ per contour length $L$. The relationship was derived for chains of uniform length. Schmidt (1984) extended these calculations and derived corresponding equations for chains with Schulz–Zimm chain length distributions.

For this procedure the non-uniformity of the chain length has to be known approximately. For the synthetic amyloses this causes no problem, since these chains have a low non-uniformity of $1/z = (M_w/M_n - 1) < 0.1$. For the various cellulose samples the Schulz–Flory distribution with $1/z = 1.0$ is a reasonable and widely accepted approximation. The data obtained for $l_k$ using these non-uniformity parameters are given in the first line of Table 2.

A second, more reliable estimation of the Kuhn-segment lengths is derived from the Koyama theory of worm-like chains (Koyama, 1973), where again the chain length non-uniformity was taken into account by Schmidt (1984). On the basis of this theory Dolega (1990) developed a special computer program, which by error minimatisation could find by an iterative process the best fit parameters for the Kuhn segment length $l_k$, the contour length $L_w$ and polydispersity $z$. The quality of the fit is best recognized in a Casassa–Holtzer plot (Casassa, 1955; Holtzer, 1955) that was first suggested and discussed in terms of physical parameters by Schmidt *et al.* (1985). In this plot the reduced scattering intensities $R_0/Kc = P(q)M_w$ is multiplied by $q$ and normalized with respect of $\pi$. Figure 4 shows the result from five celluloses and five amyloses of different chain length as examples. The full circles and shaded circles represent the experimental data, and the lines demonstrate the fits by the Koyama theory. As already mentioned the position and height of the maxima and the plateau height at large $u = qR_g$ have a simple physical meaning.

At large $u$ only the internal structure of the chain is seen. In that limit the segments can be considered as rigid rods, which in the Casassa–Holtzer plot results in an $u$-independent plateau. This plateau height gives the linear mass density $M_L = (M/L)$ of the rod like segment sections. Rigid rods develop no maximum. The ratio of the maximum height to the plateau height is a measure of the number of Kuhn segments $N_{kw}$ (weight average), and the position of the maximum depends on the non-uniformity. For uniform chain length the maximum occurs at $u = 1.41$ and it moves to larger $u$ with increasing non-uniformity and reaches a value of $u = 1.71$ when $1/z = 1.0$ (most probable Schulz–Flory distribution).

**Table 1. Weight average $M_w$, radius of gyration $R_{gz} = \langle S^2 \rangle_z^{1/2}$ and the second virial coefficient $A_2$ of celluloses and amyloses in FeTNa**

| Sample | $M_w$ (g/mol) | $R_g$ (nm) | $A_2$ (mol·ml/g$^2$) |
|---|---|---|---|
| LIN 2 | 162000 | 47 | $1.66 \cdot 10^{-3}$ |
| LIN 3 | 1310000 | 153 | $2.10 \cdot 10^{-3}$ |
| TE 69 | 155000 | 46 | $2.54 \cdot 10^{-3}$ |
| TE 72 | 202000 | 54 | $2.35 \cdot 10^{-3}$ |
| CEL 2 | 258000 | 73 | $2.28 \cdot 10^{-3}$ |
| CEL 3 | 243000 | 67 | $1.26 \cdot 10^{-3}$ |
| CEL 5 | 290000 | 73 | $1.89 \cdot 10^{-3}$ |
| CEL 6 | 684000 | 103 | $1.91 \cdot 10^{-3}$ |
| CEL 7 | 460000 | 97 | $1.80 \cdot 10^{-3}$ |
| A 1 | 105000 | 28 | $1.70 \cdot 10^{-3}$ |
| A 2 | 128000 | 34 | $1.83 \cdot 10^{-3}$ |
| A 3 | 177000 | 39 | $1.57 \cdot 10^{-3}$ |
| A 4 | 294000 | 54 | $9.16 \cdot 10^{-3}$ |
| A 5 | 422000 | 66 | $9.68 \cdot 10^{-3}$ |
| A 6 | 473000 | 76 | $1.55 \cdot 10^{-3}$ |

CEL: pulp celluloses.
LIN, TE: cotton linters.
A: synthetic amyloses.

**Table 2. Chain stiffness parameters of cellulose and amylose in FeTNa**

| | $l_k$ from Koyama-theory | $l_k$ calculated from $R_g$ |
|---|---|---|
| Cellulose | (19.9±1.8) nm | (22.4±3.5) nm |
| Amylose | (18.1±3.0) nm | (17.7±2.6) nm |

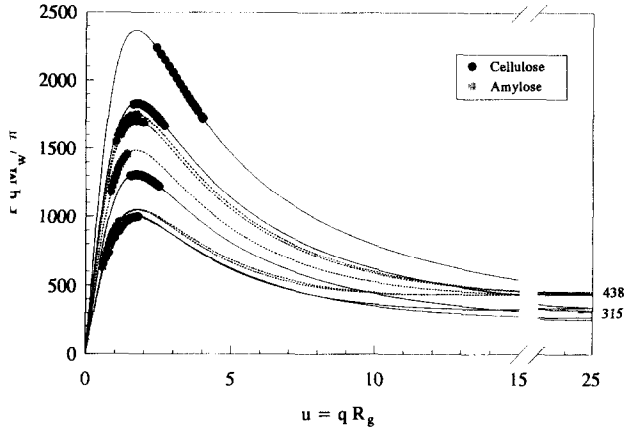


**Fig. 4.** Casassa–Holtzer-plot for five cellulose and five amylose samples. The solid and dashed lines represent the calculated fit curves.

We start the discussion with the plateau height. Assuming an effective bond length of $l_0 = 0.515$ nm for cellulose (Fengel & Wegener, 1989) and $l_0 = 0.37$ nm for amylose (Zugenmaier & Sarko, 1980) one obtains values of $M_L = (M_0/l_0) = 315$ g/(nm mol) for cellulose and $M_L = 438$ g/(nm mol) for amylose. The fits give a reasonable agreement. The fairly large error arising, of course, from the fairly short section, that could be covered by the experimental data,

nevertheless confirms that only single chains are present which appear not being 'substituted' by the complexing agent. Thus FeTNa behaves differently from cuoxam, where a much stronger complexation was found, resulting in a cellulose chain, that seems to be derivatized by a copper–ammonia-substituent (Seger & Burchard, 1994).

We next discuss the chain stiffness. The Kuhn segment lengths of the two chains appear within the limits of error to be about the same with a slight tendency to a somewhat larger one for cellulose. Commonly the Kuhn segment length is taken as a measure of chain rigidity. However, such simplifying consideration is applicable only for carbon–carbon chains. A more precise measure is the number of monomeric units per Kuhn segment, since this number is directly connected with the bond correlation $\langle \underline{l}_1 \cdot \underline{l}_n \rangle / l^2 = e^{-2}$, where $\underline{l}_1$ and $\underline{l}_n$ denote the bond vectors at the two ends of a Kuhn segment. With the effective bond lengths of $l_0 = 0.515$ nm for cellulose and $l_0 = 0.37$ nm for amylose we now obtain the numbers of 40±4 units per $l_k$ for cellulose and 48±6 for amylose. Again these numbers are within errors not distinguishable, but still the amylose has a tendency to a stronger hindrance to rotation. These findings are in good agreement with old data obtained for the carbanilate derivatives (Burchard & Husemann, 1961; Burchard, 1971). These derivatives show almost the same properties as found for the unsubstituted chains in FeTNa.

*Excluded volume effect*

So far, the excluded volume effect has been neglected. For good solvents this effect becomes noticeable for long polymer chains and would result in an overestimation of the chain stiffness. The effect of excluded volume can be estimated from the magnitude of the second virial coefficient $A_2$, the molar mass $M_w$ and the radius of gyration $R_g$. According to Yamakawa (1971) an interpenetration function $\Psi(z)$, can be calculated using the relationship

$$\Psi(z) = A_2 M_w^2 / (4\pi^{3/2} N_L R_g^3) \qquad (2)$$

Figure 5 shows the plot of $\Psi(z)$ as a function of the molar mass for cellulose and amylose in FeTNa. For random coils of flexible chains $\Psi(z)$ approaches a plateau at $\Psi(z)^* = 0.24$ (Freed, 1987). Lower values indicate better interpenetration or weaker influence of the excluded volume. For all the samples examined we obtained $\Psi$-values in a range of 0.02 to 0.07, in good agreement with the results by Valtasaari (1972) with $\Psi(z) = 0.1$. Kamide and Saito (1983) checked the literature data for cellulose in FeTNa by applying various theories. He found, that the excluded volume effect has only a little influence on the chain expansion. This conclusion is in good agreement with a comment by Fujita (1988), who concluded that the excluded volume effect becomes effective and noticeable only for chains longer than $50\,l_k$.

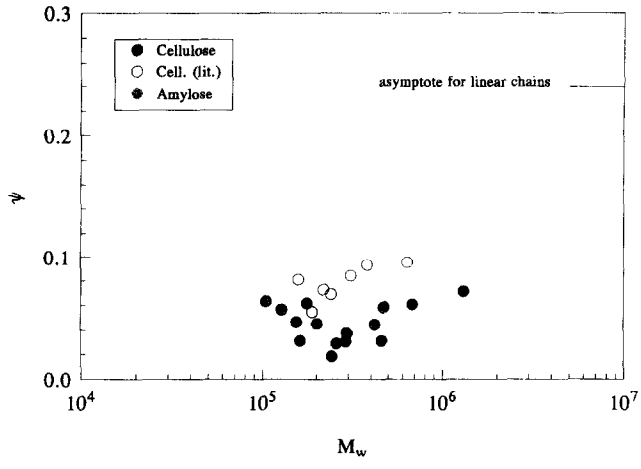


**Fig. 5.** Interpenetration function $\Psi(z)$ as a function of molar mass. The solid line represents the plateau for random coils of flexible chains.

**Semidilute concentration regime**

In the dilute concentration regime the behaviour of isolated polysaccharide chains could be investigated. When the polymer concentration reaches the overlap concentration $c^*$ the chains start to come into contact, and coupled multi-chain behaviour becomes apparent. Above $c^*$ non-polar, flexible chains interpenetrate and lead to a transient network of entangled chains (de Gennes, 1979; des Cloiseaux, 1975).

Because of the many OH-groups the entanglement formation of polysaccharides is often accompanied by association phenomena. Such association is easily detected by a strong increase in the apparent molar mass $M_{app}(c)$ that is measured at the concentration $c$. Figure 6 shows a Guinier-plot of the light scattering data for an amylose sample in FeTNa up to a concen-

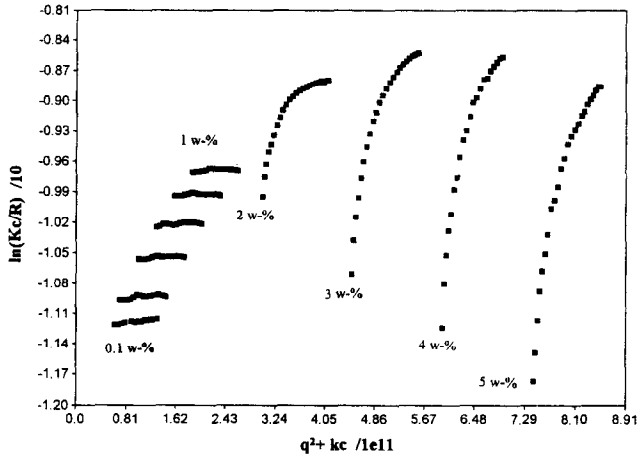


**Fig. 6.** Guinier-plot ($\ln(Kc/R_\theta)$ against $q^2 + kc$) for amylose sample A-1 in FeTNa ($c = 0.1$–$5.0$ w-%). Above 2 w-% a strong angular dependence indicates the onset of association.

molar mass $1/M_{app}(c)$. According to theory the apparent molar mass is given by the equation

$$\frac{1}{M_{app}(c)} = \frac{1}{M_w(c)} \cdot [1 + 2A_2 M_{app}(c)c + 3A_3 M_w(c)c^2 + \ldots] \quad (3)$$

Thus the reciprocal molar mass should increase with increasing concentration. This is only found up to a certain concentration and evidently an anomalous behaviour occurs around a concentration of $c$ = 1–2%.

Extrapolation to infinite dilution is no longer possible. However, all curves can be extrapolated to zero scattering angle, which provides the reduced osmotic modulus $(M_w/RT)\cdot\partial\pi/\partial c$.

$$M_w Kc/R_{\theta=0} = M_w/M_{app} = (M_w/RT)\partial\pi/\partial c \quad (4)$$

The concentration dependence of the reduced osmotic modulus was studied previously with a number of different macromolecular architectures (Burchard, 1988, 1990; Burchard *et al.*, 1992), and in all cases the parameter

$$X = A_2 M_w c \equiv c/c^* \quad (5)$$

was found to be an efficient scaling parameter. The osmotic modulus could be described in terms of these parameters, but different curves were obtained for the various structures. Hence various structures can be distinguished by their strength of intermolecular interactions. With these results in mind the findings shown in Fig. 7 become interesting.

Both chains in FeTNa initially follow the curve as predicted by Ohta and Oono (1983) for flexible coils. The second theoretical curve in Fig. 7 represents the osmotic modulus for hard spheres referring to Carnahan and Starling (1969). At about $2X$ ($c^*$ = 5.6 g/l) a sudden departure from the flexible coil line occurs for amylose, for cellulose this is observed much earlier at about $0.2X$ ($c^*$ = 3.7 g/l). Inspection of eq. (3) reveals that such inversion of the curve can happen only when $M_w(c)$ increases more strongly with $c$ than the repulsive osmotic modulus. Apparently a strong association occurs around the overlap concentration for amylose and much earlier already for cellulose. This association process goes on for amylose with increasing $c$ until $1/M_w(c)$ reaches a value zero which means divergence of $M_w(c)$, or the approach of a reversible gel-point.

Cellulose behaves differently in this solvent. The association process starts earlier but remains then on an intermediate stage up to $c = 8c^*$, where $c^*$ is based on the non-associated molar mass. Similar behaviour was recently observed by Stock *et al.* (1992) with styrene-co-isoprene chains which were substituted with urazole groups. These groups can undergo H-bond formation, which will happen predominantly intramolecularly, already when the concentration is much lower than the overlap concentration. For the present cellulose such

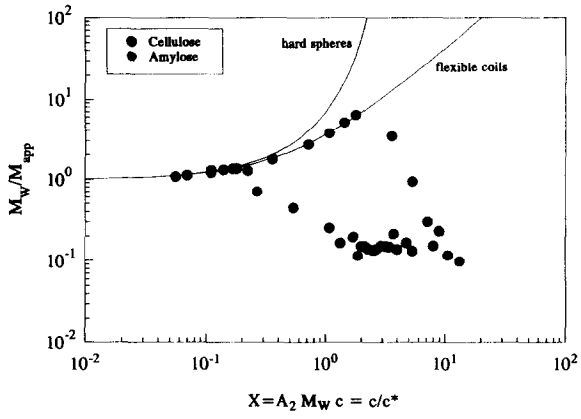


**Fig. 7.** Reduced osmotic modulus as a function of the parameter $X = A_2 M_w c$ for amylose sample A-1 and cellulose sample LIN-2 in FeTNa. The full lines represent theoretical curves for hard spheres by Carnahan and Starling and flexible chains by Ohta and Oono.

microgel formation is less likely than a kind of micellation for the following reason. Native cellulose is known to have a partially crystalline fibrous structure. Therefore, the dissolution process will start in the less ordered fibre region leaving the crystalline domains essentially unchanged. The resulting structure will resemble a fringed micelle with at least 10 side-by-side aggregated chains and about twice as many flexible outer chain sections (compare Ebringerova *et al.*, 1994).

A similar structure is not expected for amylose since this chain dissolves already in sodium hydroxide and has no long crystalline sections, if retrogradation of the amylose was prevented.

These conclusions, drawn from the intermolecular interactions as measured by static LS, could be confirmed by dynamic LS. Interest was focussed on the investigation of the semi-diluted concentration regime. The determination of hydrodynamic radii $R_h$ was involved with problems already in highly diluted solutions, which were caused by colloidal particles of FeTNa and a small amount of aggregates as mentioned above. These particles led to severe distortions of the time correlation functions $g_1(t)$, in particular if the polymer concentration is below the overlap concentration. The time correlation function $g_1(t)$ displays two and often three relaxation processes for both polysaccharides, as demonstrated in Fig. 8 for the scattering angle of 90°. With increasing concentrations, the slow modes of motion are shifted to longer relaxation times, and this is accompanied by a strong increase of the amplitude. The fast motion may be interpreted as the common collection diffusion, or as the typical gel mode. The slowest motion is probably due to a diffusive migration of heterogeneities that may be caused by random dissociation or association of chains to a large cluster. The observed motion in between these two may arise from the translational diffusion of aggregates, which are present even in highly diluted solutions and

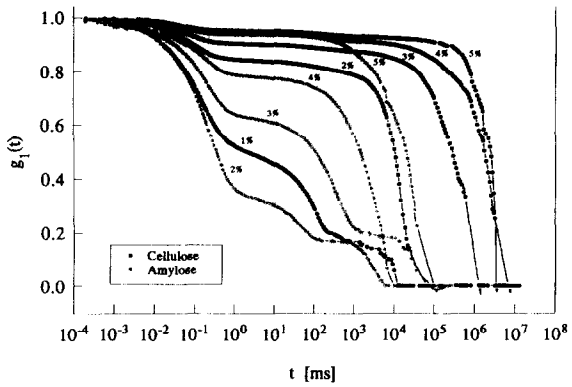


**Fig. 8.** Time correlation function $g_1(t) = \langle E(0)\, E(t)\rangle / \langle E(0)\rangle^2$ for amylose sample A-1 and cellulose sample LIN-2 at a scattering angle of 90°.

grow as association proceeds with increasing concentration.

A closer inspection of Fig. 8 reveals a significant difference in behaviour of the cellulose and amylose chains. The intermediate slow motion is considerably more strongly slowed down for cellulose than for amylose and becomes predominant already at $c \ll c^*$. This observation is consistent with the static properties and indicates an association for cellulose well before $c^*$ is reached.

This leads to the conclusion, that in the case of amylose, an entanglement network is built up mainly by single chains, that becomes fixed for a certain lifetime. Cellulose seems to form a transient network consisting of fringed micellar aggregates in solution, which are entangled by the flexible arms of these aggregates and are again temporarily fixed via H-bonds. The described solution behaviour above the overlap concentration is represented in Fig. 9. The indicated highly ordered core of the fringed micelles of cellulose and its derivatives in solution is actually observed and investigated in various solvent systems (Burchard & Schulz, 1995). Further details will be published elsewhere.

## CONCLUSION

The iron tartaric acid complex solvent FeTNa offered the possibility for a direct comparison of the solution properties of cellulose and amylose. No significant difference in the dilute solution behaviour was noticed. The Kuhn segment length of $l_k$ = 21.6 (±3.6) nm for cellulose and 17.4 (±2.7) nm for amylose, respectively, demonstrates a considerable chain stiffness that corresponds well to the findings with the carbanilate derivatives in dioxan. The linear mass densities $M_L$ agree with those for single stranded chains and led to the conclusion, that the polysaccharide chains are not 'substituted' by the iron complex in the sense of a derivatization. In this complex equilibrium the high sodium hydroxide concentration has the function of an activating medium.

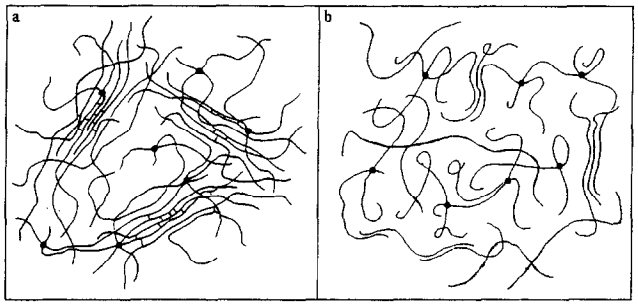


**Fig. 9.** Suggested solution structure for concentrations above the overlap concentration $c^*$ of (a) cellulose and (b) amylose in FeTNa.

Remarkable differences were found, however, when increasing the polymer concentration. Amylose behaves as a common flexible coil up to about two times the overlap concentration. Then an onset of association takes place. Cellulose, on the other hand, starts already to associate well before reaching the overlap concentration. It exhibits a metastable intermediate association state that is typical for micellar structures. These findings could be confirmed by the analysis of the time correlation functions, which exhibit a pronounced slow motion in addition to the common fast one. The fibrous structure of cellulose, preformed by the β-(1.4) linkage, apparently causes severe dissolution problems. Although FeTNa seems not to be able to break up the crystalline fibre regions, visually clear solutions are obtained. The non crystalline structure of the α-(1.4) linked amylose causes a better solubility and favours a better penetration of the chains. Beyond $c^*$ the entangled transient network becomes partially fixed by associating H-bonds which leads to large clusters and eventually to reversible gel formation.

## REFERENCES

Baur, G. (1990). *Special development of SLS-Systemtechnik*, Hausen.

Benoit, H. & Doty, P.(1953). *J. Chem. Phys.*, **57,** 958.

Burchard, W. (1965). *Macromol. Chem.*, **88,** 11–28.

Burchard, W. (1971). *Br. Polym. J.*, **3,** 214.

Burchard, W. (1988). *Macromol. Chem., Macromol. Sympos.*, **18,** 1.

Burchard, W. (1990). *Macromol. Chem., Macromol. Sympos.*, **39,** 179.

Burchard, W. & Husemann, E. (1961). *Macromol. Chem.*, **44–46,** 358–387.

Burchard, W., Lang, P., Schulz, L. & Coviello, T. (1992). *Macromol. Chem., Macromol. Sympos.*, **58,** 21.

Burchard, W. (1993). Solution properties of plant polysaccharides as a function of their chemical structure. In *Plant Polymeric Carbohydrates*, Meuser, F., Manners, G.J., Seibel, W., The Royal Society of Chemistry, Cambridge.

Burchard, W., Schulz, L. (1995). *Macromol. Chem. Macromol. Sympos.*, **99,** 57–69.

Carnahan, N.F. & Starling, K.E. (1969). *J. Chem. Phys.*, **51,** 635.

Casassa, E.F. (1955). *J. Phys. Chem.*, **23,** 596.
des Cloiseaux, J. (1975). *J. Physique,* **36,** 281.
Dandliker, W.B. & Kraut, J. (1956). *J. Am. Chem. Soc.*, **78,** 2380–2384.
Denkinger, P. & Burchard, W. (1991). *J. Polym. Sci., Part B: Polym. Phys.*, **29,** 589.
Dolega, U. & Denkinger, P. (1990). Computer program, developed at University of Freiburg.
Ebringerova, A., Hromadkova, Z., Dolega, R., Burchard, W. & Vorwerg, W. (1994). *Carbohydr. Polym.*, **24,** 161–169.
Fengel, D. & Wegener, G. (1989). *Wood Chemistry, Ultrastructure, Reactions.* Walter de Gruyter, Berlin.
Freed, K. F. (1987). *Renormalization Group Theory of Macromolecules.* Wiley, New York.
Fujita, H. (1988). *Macromolecules,* **17,** 553.
de Gennes, P.G. (1979). *Scaling Concepts in Polymer Physics.* Cornell University Press, Itaka, New York.
Holtzer, A.F. (1955). *J. Polym. Sci.*, **17,** 433.
Jayme, G. & Bergmann, W. (1956). *Das Papier,* **10,** 307.
Kamide, K. & Saito, M. (1983). *Macromol. Chem., Rapid Commun.*, **4,** 33–39.
Koyama, R. (1973). *J. Phys. Soc. Jpn.*, **34,** 1029.
Ohta, T. & Oono, Y. (1983). *Phys. Lett.*, **79,** 339.
Pfannemüller, B. & Burchard, W. (1969). *Macromol. Chem.*, **121,** 1–17.
Schmidt, M. (1984). *Macromolecules,* **17,** 553.
Schmidt, M., Paradossi, G. & Burchard, W.(1985). *Macromol. Chem., Rapid. Commun.*, **6,** 767.
Seger, B. & Burchard, W. (1994). *Macromol. Symp.*, **83,** 291–310.
Stock, J., Burchard, W. & Stadler, R. (1992). *Macromolecules,* **25,** 6885.
Valtasaari, L. (1957). *Paperi ja Puu,* **4,** 243–252.
Valtasaari, L. (1971). *Macromol. Chem.*, **150,** 117–126.
Yamakawa, H. (1971). *Modern Theory of Polymer Solutions.* Harper and Row, New York.
Zugenmaier, P., Sarko, A. (1980). The variable virtual bond. Modeling technique for solving polymer crystal structures. In *Fiber diffraction methods. ACS Symposium Series 141,* French, A. & Gardner, K.H. (eds). American Chemical Society, Washington DC, pp. 225–238.